
Supplementary Material:
T-ESKF: Transformed Error-State Kalman Filter for
Consistent Visual-Inertial Navigation

Chungeng Tian
Ning Hao
Fenghua He

2024-06

Contents

1 Structure of This Supplementary Material	3
2 Preliminary: Special Orthogonal Group	3
2.1 Lie algebra	3
2.2 Exponential and logarithmic map	3
2.3 Adjoint operation	4
2.4 Jacobians	4
3 IMU Model and error-state kinematics	5
3.1 IMU model	5
3.2 IMU state estimate and error-state	5
3.3 IMU error-state kinematics	6
3.3.1 Orientation	7
3.3.2 Position	7
3.3.3 Velocity	8
3.3.4 Bias	8
4 Visual-Inertial Navigation System	8
4.1 System model	8
4.2 Linearized error-state system	9
5 Transformed Linearized Error-State System	11
5.1 Linear time-varying transformation on error-state	11
5.2 Observability of the transformed system	12
6 Transformed Error-State Kalman Filter	14
6.1 Propagation	14
6.2 Update	15
6.3 Inverse transformation	16
6.4 Initialization	16
7 Real-World Experiments	17
A Derivation of $C_2 = [g]_\times$	20

1 Structure of This Supplementary Material

The relation between this supplementary material and the manuscript is displayed in Figure 1. In this supplementary material, Section 2 provides the basic knowledge of $\mathbf{SO}(3)$. Sections 3-6 present the model and method encompassing the consideration of IMU bias. The real-world experiments on our custom platform are given in Section 7. Appendix A contains the derivation of $\mathbf{C}_2 = [\mathbf{g}]_\times$, which is omitted in the manuscript.

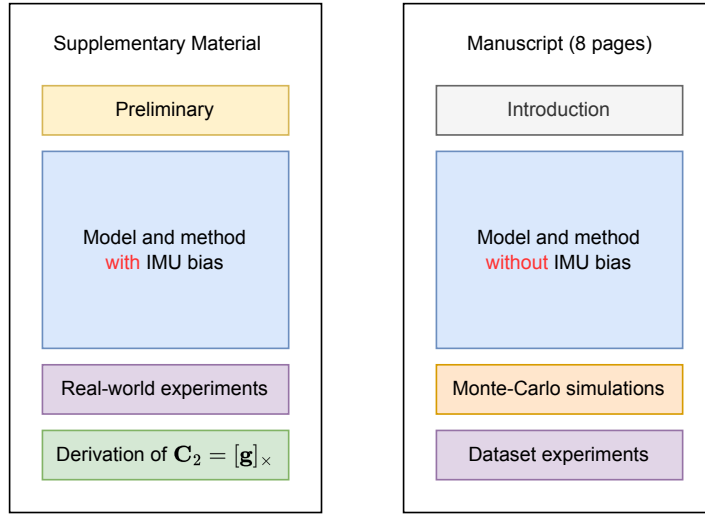


Figure 1: Relation between this supplementary material and the manuscript.

2 Preliminary: Special Orthogonal Group

2.1 Lie algebra

The Lie algebra corresponding to $\mathbf{SO}(3)$ is

$$\mathfrak{so}(3) = \{\boldsymbol{\theta}^\wedge | \boldsymbol{\theta} \in \mathbb{R}^3\}. \quad (1)$$

For $\mathbf{SO}(3)$, $\boldsymbol{\theta}^\wedge = [\boldsymbol{\theta}]_\times$ with

$$[\boldsymbol{\theta}]_\times = \begin{bmatrix} \theta_1 \\ \theta_2 \\ \theta_3 \end{bmatrix}_\times = \begin{bmatrix} 0 & -\theta_3 & \theta_2 \\ \theta_3 & 0 & -\theta_1 \\ -\theta_2 & \theta_1 & 0 \end{bmatrix} \quad (2)$$

2.2 Exponential and logarithmic map

Let $\boldsymbol{\theta}$ represent a rotation, where $\theta \triangleq |\boldsymbol{\theta}|$ is the rotation angular and $\mathbf{u} \triangleq \frac{\boldsymbol{\theta}}{|\boldsymbol{\theta}|}$ is the rotation axis. The exponential map $\exp : \mathfrak{so}(3) \rightarrow \mathbf{SO}(3)$ from the space of $\mathfrak{so}(3)$ to the space of the rotations represented by

rotation matrices is

$$\exp([\boldsymbol{\theta}]_{\times}) = \mathbf{I}_3 + \frac{1}{1!} [\boldsymbol{\theta}]_{\times} + \frac{1}{2!} [\boldsymbol{\theta}]_{\times}^2 + \frac{1}{3!} [\boldsymbol{\theta}]_{\times}^3 + \dots \quad (3a)$$

$$= \mathbf{I}_3 + \left(\frac{\theta}{1!} - \frac{\theta^3}{3!} + \frac{\theta^5}{5!} - \dots \right) [\mathbf{u}]_{\times} + \left(\frac{\theta^2}{2!} - \frac{\theta^4}{4!} + \frac{\theta^6}{6!} - \dots \right) [\mathbf{u}]_{\times}^2 \quad (3b)$$

$$= \mathbf{I}_3 + \sin\theta [\mathbf{u}]_{\times} + (1 - \cos\theta) [\mathbf{u}]_{\times}^2 \quad (3c)$$

$$= \mathbf{I}_3 \cos\theta + [\mathbf{u}]_{\times} \sin\theta + \mathbf{u}\mathbf{u}^{\top} (1 - \cos\theta) \quad (3d)$$

$$\triangleq \mathbf{R} \quad (3e)$$

The exponential map $\text{Exp} : \mathbb{R}^3 \rightarrow \mathbf{SO}(3)$ is defined as

$$\text{Exp}(\boldsymbol{\theta}) = \exp([\boldsymbol{\theta}]_{\times}) \quad (4)$$

The logarithmic map is defined as the inverse of the exponential map with $\log : \mathbf{SO}(3) \rightarrow \mathfrak{so}(3) = [\mathbf{u}\theta]_{\times}$ and $\text{Log} : \mathbf{SO}(3) \rightarrow \mathbb{R}^3 = \mathbf{u}\theta$, where

$$\theta = \arccos\left(\frac{\text{trace}(\mathbf{R}) - 1}{2}\right) \quad (5)$$

$$\mathbf{u} = \frac{(\mathbf{R} - \mathbf{R}^{\top})^{\vee}}{2 \sin \theta} \quad (6)$$

and $(\cdot)^{\vee}$ is the inverse of $(\cdot)^{\wedge}$.

2.3 Adjoint operation

If $\phi \in \mathbb{R}^3$, the adjoint operation for $\mathbf{R} \in \mathbf{SO}(3)$ is defined as

$$\mathbf{R}[\phi]_{\times} \mathbf{R}^{\top} = [Ad_{\mathbf{R}}\phi]_{\times} \quad (7)$$

$$\mathbf{R}\text{Exp}(\phi)\mathbf{R}^{\top} = \text{Exp}(Ad_{\mathbf{R}}\phi) \quad (8)$$

$$Ad_{\mathbf{R}} = \mathbf{R} \quad (9)$$

2.4 Jacobians

Assuming that ϕ is small enough, we have

$$\text{Exp}(\boldsymbol{\theta} + \phi) \approx \text{Exp}(\boldsymbol{\theta})\text{Exp}(\mathbf{J}_r(\boldsymbol{\theta})\phi) \quad (10)$$

$$\text{Exp}(\boldsymbol{\theta} + \phi) \approx \text{Exp}(\mathbf{J}_l(\boldsymbol{\theta})\phi)\text{Exp}(\boldsymbol{\theta}) \quad (11)$$

where

$$\mathbf{J}_r(\boldsymbol{\theta}) = \frac{\sin\theta}{\theta} \mathbf{I}_3 + \left(1 - \frac{\sin\theta}{\theta}\right) \mathbf{u}\mathbf{u}^{\top} - \frac{1 - \cos\theta}{\theta} [\mathbf{u}]_{\times} \quad (12)$$

and $\mathbf{J}_l(\boldsymbol{\theta}) = \mathbf{J}_r(-\boldsymbol{\theta})$. \mathbf{J}_r and \mathbf{J}_l are called right and left Jacobians of $\mathbf{SO}(3)$, respectively.

3 IMU Model and error-state kinematics

This section presents the IMU model and its error-state kinematics. The main result is equivalent to *The ESKF using global angular errors* [1, Chapter 7]. If you are familiar with ESKF, you can skip this section.

3.1 IMU model

The IMU state vector is

$$\mathbf{x}_I = (\mathbf{R}, \mathbf{p}, \mathbf{v}, \mathbf{b}_g, \mathbf{b}_a) \quad (13)$$

where $\mathbf{R} \in \mathbf{SO}(3)$, $\mathbf{p} \in \mathbb{R}^3$ and $\mathbf{v} \in \mathbb{R}^3$ are the orientation, position, and velocity of IMU in the global frame. $\mathbf{b}_g \in \mathbb{R}^3$ and $\mathbf{b}_a \in \mathbb{R}^3$ are the gyroscope bias and accelerometer bias.

The continuous motion model is

$$\dot{\mathbf{R}} = \mathbf{R} [\boldsymbol{\omega}]_\times \quad (14a)$$

$$\dot{\mathbf{p}} = \mathbf{v} \quad (14b)$$

$$\dot{\mathbf{v}} = \mathbf{a} \quad (14c)$$

$$\dot{\mathbf{b}}_g = \mathbf{n}_{gw} \quad (14d)$$

$$\dot{\mathbf{b}}_a = \mathbf{n}_{aw} \quad (14e)$$

where

$$\boldsymbol{\omega} = \boldsymbol{\omega}_m - \mathbf{b}_g - \mathbf{n}_g \quad (15)$$

$$\mathbf{a} = \mathbf{R}(\mathbf{a}_m - \mathbf{b}_a - \mathbf{n}_a) + \mathbf{g} \quad (16)$$

$\boldsymbol{\omega}_m \in \mathbb{R}^3$ and $\mathbf{a}_m \in \mathbb{R}^3$ are the gyroscope and accelerometer measurements in the IMU frame, $\mathbf{n}_{gw} \sim \mathcal{N}(0, \sigma_{gw}^2 \mathbf{I}_3)$, $\mathbf{n}_{aw} \sim \mathcal{N}(0, \sigma_{aw}^2 \mathbf{I}_3)$, $\mathbf{n}_g \sim \mathcal{N}(0, \sigma_g^2 \mathbf{I}_3)$, and $\mathbf{n}_a \sim \mathcal{N}(0, \sigma_a^2 \mathbf{I}_3)$ are white Gaussian noises.

3.2 IMU state estimate and error-state

Let $\hat{\mathbf{x}}_I$ denote the IMU state estimate, which is propagated following (14) by setting the process noise to zero:

$$\dot{\hat{\mathbf{R}}} = \hat{\mathbf{R}} [\hat{\boldsymbol{\omega}}]_\times \quad (17a)$$

$$\dot{\hat{\mathbf{p}}} = \hat{\mathbf{v}} \quad (17b)$$

$$\dot{\hat{\mathbf{v}}} = \hat{\mathbf{a}} \quad (17c)$$

$$\dot{\hat{\mathbf{b}}}_g = \mathbf{0} \quad (17d)$$

$$\dot{\hat{\mathbf{b}}}_a = \mathbf{0} \quad (17e)$$

with

$$\hat{\omega} = \omega_m - \hat{\mathbf{b}}_g \quad (18)$$

$$\hat{\mathbf{a}} = \hat{\mathbf{R}}(\mathbf{a}_m - \hat{\mathbf{b}}_a) + \mathbf{g}. \quad (19)$$

In ESKF, the error-state of orientation is defined using the logarithm of $\mathbf{SO}(3)$ while the errors of other variables are defined on vector space:

$$\tilde{\mathbf{x}}_I = \mathbf{x}_I \ominus \hat{\mathbf{x}}_I \quad (20)$$

where the general minus \ominus is defined as

$$\tilde{\boldsymbol{\theta}} = \text{Log}(\mathbf{R}\hat{\mathbf{R}}^{-1}) \quad (21a)$$

$$\tilde{\mathbf{p}} = \mathbf{p} - \hat{\mathbf{p}} \quad (21b)$$

$$\tilde{\mathbf{v}} = \mathbf{v} - \hat{\mathbf{v}} \quad (21c)$$

$$\tilde{\mathbf{b}}_g = \mathbf{b}_g - \hat{\mathbf{b}}_g \quad (21d)$$

$$\tilde{\mathbf{b}}_a = \mathbf{b}_a - \hat{\mathbf{b}}_a \quad (21e)$$

3.3 IMU error-state kinematics

The IMU error-state kinematics is

$$\dot{\tilde{\boldsymbol{\theta}}} = -\hat{\mathbf{R}}\mathbf{b}_g - \hat{\mathbf{R}}\mathbf{n}_g \quad (22a)$$

$$\dot{\tilde{\mathbf{p}}} = \tilde{\mathbf{v}} \quad (22b)$$

$$\dot{\tilde{\mathbf{v}}} = -\left[\hat{\mathbf{R}}(\mathbf{a}_m - \hat{\mathbf{b}}_a)\right]_{\times} \tilde{\boldsymbol{\theta}} - \hat{\mathbf{R}}\tilde{\mathbf{b}}_a - \hat{\mathbf{R}}\mathbf{n}_a \quad (22c)$$

$$\dot{\tilde{\mathbf{b}}}_g = \mathbf{n}_{gw} \quad (22d)$$

$$\dot{\tilde{\mathbf{b}}}_a = \mathbf{n}_{aw} \quad (22e)$$

The derivation of the equations is given in Section 3.3.1-3.3.4. The above equations can be written in matrix form:

$$\dot{\tilde{\mathbf{x}}}_I = \mathbf{F}_I \tilde{\mathbf{x}}_I + \mathbf{G}_I \mathbf{n} \quad (23)$$

where

$$\mathbf{F}_I = \begin{bmatrix} 0 & 0 & -\hat{\mathbf{R}} & 0 \\ 0 & 0 & \mathbf{I}_3 & 0 \\ -[\hat{\mathbf{R}}(\mathbf{a}_m - \hat{\mathbf{b}}_a)]_\times & 0 & 0 & -\hat{\mathbf{R}} \\ 0 & 0 & 0 & 0 \\ 0 & 0 & 0 & 0 \end{bmatrix}, \quad (24)$$

$$\mathbf{G}_I = \begin{bmatrix} -\hat{\mathbf{R}} & 0 & 0 & 0 \\ 0 & 0 & 0 & 0 \\ 0 & -\hat{\mathbf{R}} & 0 & 0 \\ 0 & 0 & \mathbf{I} & 0 \\ 0 & 0 & 0 & \mathbf{I} \end{bmatrix}, \quad (25)$$

$$\mathbf{n} = \begin{bmatrix} \mathbf{n}_g \\ \mathbf{n}_a \\ \mathbf{n}_{gw} \\ \mathbf{n}_{aw} \end{bmatrix}, \quad (26)$$

with $\mathbf{E}(\mathbf{n}\mathbf{n}^\top) = \mathbf{Q}$.

3.3.1 Orientation

$$\begin{aligned} \left(\text{Exp}(\tilde{\boldsymbol{\theta}})\hat{\mathbf{R}} \right) &= \dot{\mathbf{R}} = \mathbf{R}[\boldsymbol{\omega}]_\times \\ \text{Exp}(\tilde{\boldsymbol{\theta}})\hat{\mathbf{R}} + \text{Exp}(\tilde{\boldsymbol{\theta}})\dot{\hat{\mathbf{R}}} &= = \left(\text{Exp}(\tilde{\boldsymbol{\theta}})\hat{\mathbf{R}} \right)[\boldsymbol{\omega}]_\times \\ \text{Exp}(\tilde{\boldsymbol{\theta}})\left[\dot{\tilde{\boldsymbol{\theta}}} \right]_\times \hat{\mathbf{R}} + \text{Exp}(\tilde{\boldsymbol{\theta}})\hat{\mathbf{R}}[\dot{\boldsymbol{\omega}}]_\times &= = \text{Exp}(\tilde{\boldsymbol{\theta}})\hat{\mathbf{R}}[\boldsymbol{\omega}]_\times \end{aligned} \quad (27)$$

Having $\boldsymbol{\omega} - \dot{\boldsymbol{\omega}} = -\tilde{\mathbf{b}}_g - \mathbf{n}_g$, this reduces to

$$\left[\dot{\tilde{\boldsymbol{\theta}}} \right]_\times \hat{\mathbf{R}} = \hat{\mathbf{R}} \left[-\tilde{\mathbf{b}}_g - \mathbf{n}_g \right]_\times \quad (28)$$

Right-multiplying left and right terms by $\hat{\mathbf{R}}^{-1}$, and recalling the adjoint operation on $\mathbf{SO}(3)$, i.e., (7), we have

$$\left[\dot{\tilde{\boldsymbol{\theta}}} \right]_\times = \hat{\mathbf{R}} \left[-\tilde{\mathbf{b}}_g - \mathbf{n}_g \right]_\times \hat{\mathbf{R}}^{-1} \quad (29)$$

$$= \left[-\hat{\mathbf{R}}\tilde{\mathbf{b}}_g - \hat{\mathbf{R}}\mathbf{n}_g \right]_\times \quad (30)$$

Finally, the error-state kinematic equation for orientation is given by

$$\dot{\tilde{\boldsymbol{\theta}}} = -\hat{\mathbf{R}}\tilde{\mathbf{b}}_g - \hat{\mathbf{R}}\mathbf{n}_g \quad (31)$$

3.3.2 Position

$$\begin{aligned} (\hat{\mathbf{p}} + \tilde{\mathbf{p}}) &= \dot{\mathbf{p}} = \mathbf{v} \\ \hat{\mathbf{v}} + \dot{\tilde{\mathbf{p}}} &= = \hat{\mathbf{v}} + \tilde{\mathbf{v}}. \end{aligned} \quad (32)$$

The position error-state kinematics is :

$$\dot{\tilde{\mathbf{p}}} = \tilde{\mathbf{v}} \quad (33)$$

3.3.3 Velocity

$$\begin{aligned} (\hat{\mathbf{v}} + \tilde{\mathbf{v}}) &= \dot{\mathbf{v}} = \mathbf{a} \\ \hat{\mathbf{a}} + \dot{\tilde{\mathbf{v}}} &= \mathbf{R}(\mathbf{a}_m - \mathbf{b}_a - \mathbf{n}_a) + \mathbf{g} \\ \hat{\mathbf{R}}(\mathbf{a}_m - \hat{\mathbf{b}}_a) + \mathbf{g} + \dot{\tilde{\mathbf{v}}} &= \text{Exp}(\tilde{\boldsymbol{\theta}})\hat{\mathbf{R}}(\mathbf{a}_m - \mathbf{b}_a - \mathbf{n}_a) + \mathbf{g} \end{aligned} \quad (34)$$

Simplifying this equation yields the velocity error-state kinematics:

$$\dot{\tilde{\mathbf{v}}} = \text{Exp}(\tilde{\boldsymbol{\theta}})\hat{\mathbf{R}}(\mathbf{a}_m - \mathbf{b}_a - \mathbf{n}_a) - \hat{\mathbf{R}}(\mathbf{a}_m - \hat{\mathbf{b}}_a) \quad (35a)$$

$$\simeq \left(\mathbf{I}_3 + [\tilde{\boldsymbol{\theta}}]_{\times} \right) \text{Exp}(\tilde{\boldsymbol{\theta}})\hat{\mathbf{R}}(\mathbf{a}_m - \mathbf{b}_a - \mathbf{n}_a) - \hat{\mathbf{R}}(\mathbf{a}_m - \hat{\mathbf{b}}_a) \quad (35b)$$

$$= -\hat{\mathbf{R}}\tilde{\mathbf{b}}_a - \hat{\mathbf{R}}\mathbf{n}_a + [\tilde{\boldsymbol{\theta}}]_{\times} \hat{\mathbf{R}}(\mathbf{a}_m - \mathbf{b}_a - \mathbf{n}_a) \quad (35c)$$

$$\simeq -[\hat{\mathbf{R}}(\mathbf{a}_m - \hat{\mathbf{b}}_a)]_{\times} \tilde{\boldsymbol{\theta}} - \hat{\mathbf{R}}\tilde{\mathbf{b}}_a - \hat{\mathbf{R}}\mathbf{n}_a \quad (35d)$$

3.3.4 Bias

$$\dot{\tilde{\mathbf{b}}}_g = \dot{\mathbf{b}}_g - \dot{\tilde{\mathbf{b}}}_g = \mathbf{n}_{gw} - \mathbf{0} = \mathbf{n}_{gw} \quad (36)$$

$$\dot{\tilde{\mathbf{b}}}_a = \dot{\mathbf{b}}_a - \dot{\tilde{\mathbf{b}}}_a = \mathbf{n}_{aw} - \mathbf{0} = \mathbf{n}_{aw} \quad (37)$$

4 Visual-Inertial Navigation System

4.1 System model

The system state is

$$\mathbf{x} = (\mathbf{x}_I, \boldsymbol{\ell}) \quad (38)$$

where $\boldsymbol{\ell} \in \mathbb{R}^3$ is the landmark position in the global frame.

The system kinematic equations are

$$\dot{\mathbf{R}} = \mathbf{R}[\boldsymbol{\omega}]_{\times} \quad (39a)$$

$$\dot{\mathbf{p}} = \mathbf{v} \quad (39b)$$

$$\dot{\mathbf{v}} = \mathbf{a} \quad (39c)$$

$$\dot{\mathbf{b}}_g = \mathbf{n}_{gw} \quad (39d)$$

$$\dot{\mathbf{b}}_a = \mathbf{n}_{aw} \quad (39e)$$

$$\dot{\boldsymbol{\ell}} = \mathbf{0} \quad (39f)$$

Let ${}^I\mathbf{p}_L$ denote the landmark position in the IMU frame, expressed as

$${}^I\mathbf{p}_L = \mathbf{R}^\top(\boldsymbol{\ell} - \mathbf{p}). \quad (40)$$

As the camera explores the environment, the visual measurement of the landmark is available after the data association and rectification, formulated as

$$\mathbf{y} = \mathbf{h}({}^I\mathbf{p}_L) + \boldsymbol{\epsilon} \quad (41)$$

where $\mathbf{h} = \pi \circ \Upsilon$, $\Upsilon : \mathbb{R}^3 \rightarrow \mathbb{R}^3$ transforms points from the IMU frame to the camera frame, and $\pi : \mathbb{R}^3 \rightarrow \mathbb{R}^2$ is the camera perspective projection function, $\boldsymbol{\epsilon} \in \mathbb{R}^2$ is the zero-mean Gaussian noise with $\mathbf{E}(\boldsymbol{\epsilon}\boldsymbol{\epsilon}^\top) = \mathbf{V}$.

4.2 Linearized error-state system

Let $\hat{\mathbf{x}}$ denote the VINS state estimate, which is propagated following (39) by setting the process noise to zero:

$$\dot{\hat{\mathbf{R}}} = \hat{\mathbf{R}} [\hat{\boldsymbol{\omega}}]_\times \quad (42a)$$

$$\dot{\hat{\mathbf{p}}} = \hat{\mathbf{v}} \quad (42b)$$

$$\dot{\hat{\mathbf{v}}} = \hat{\mathbf{a}} \quad (42c)$$

$$\dot{\hat{\mathbf{b}}}_g = \mathbf{0} \quad (42d)$$

$$\dot{\hat{\mathbf{b}}}_a = \mathbf{0} \quad (42e)$$

$$\dot{\hat{\boldsymbol{\ell}}} = \mathbf{0} \quad (42f)$$

The error-state of VINS is

$$\tilde{\mathbf{x}} = \mathbf{x} \ominus \hat{\mathbf{x}} = \begin{bmatrix} \mathbf{x}_I \ominus \hat{\mathbf{x}}_I \\ \boldsymbol{\ell} - \hat{\boldsymbol{\ell}} \end{bmatrix} \triangleq \begin{bmatrix} \tilde{\mathbf{x}}_I \\ \tilde{\boldsymbol{\ell}} \end{bmatrix} \quad (43)$$

According to (23), the VINS error-state kinematics can be written as

$$\dot{\tilde{\mathbf{x}}} = \mathbf{F}\tilde{\mathbf{x}} + \mathbf{G}\mathbf{n} \quad (44)$$

where

$$\mathbf{F} = \begin{bmatrix} \mathbf{F}_I & \mathbf{0}_{15 \times 3} \\ \mathbf{0}_{3 \times 15} & \mathbf{0}_{3 \times 3} \end{bmatrix} = \begin{bmatrix} 0 & 0 & 0 & -\hat{\mathbf{R}} & 0 & 0 \\ 0 & 0 & \mathbf{I}_3 & 0 & 0 & 0 \\ -[\hat{\mathbf{R}}(\mathbf{a}_m - \hat{\mathbf{b}}_a)]_{\times} & 0 & 0 & 0 & -\hat{\mathbf{R}} & 0 \\ 0 & 0 & 0 & 0 & 0 & 0 \\ 0 & 0 & 0 & 0 & 0 & 0 \\ 0 & 0 & 0 & 0 & 0 & 0 \end{bmatrix} \quad (45)$$

$$\mathbf{G} = \begin{bmatrix} \mathbf{G}_I \\ \mathbf{0}_{3 \times 12} \end{bmatrix} = \begin{bmatrix} -\hat{\mathbf{R}} & 0 & 0 & 0 \\ 0 & 0 & 0 & 0 \\ 0 & -\hat{\mathbf{R}} & 0 & 0 \\ 0 & 0 & \mathbf{I} & 0 \\ 0 & 0 & 0 & \mathbf{I} \\ 0 & 0 & 0 & 0 \end{bmatrix} \quad (46)$$

The measurement residual is :

$$\tilde{\mathbf{y}} = \mathbf{y} - \mathbf{h}({}^I \hat{\mathbf{p}}_L) \quad (47a)$$

$$= \mathbf{h}({}^I \mathbf{p}_L) - \mathbf{h}({}^I \hat{\mathbf{p}}_L) + \epsilon \quad (47b)$$

$$= \frac{\partial \mathbf{h}}{\partial {}^I \mathbf{p}_L} d {}^I \mathbf{p}_L + \epsilon \quad (47c)$$

$$= \frac{\partial \mathbf{h}}{\partial {}^I \mathbf{p}_L} \left(\mathbf{R}^\top (\boldsymbol{\ell} - \mathbf{p}) - \hat{\mathbf{R}}^\top (\hat{\boldsymbol{\ell}} - \hat{\mathbf{p}}) \right) + \epsilon \quad (47d)$$

$$\simeq \frac{\partial \mathbf{h}}{\partial {}^I \mathbf{p}_L} \left(\hat{\mathbf{R}}^\top (\mathbf{I}_3 - [\tilde{\boldsymbol{\theta}}]_{\times}) (\boldsymbol{\ell} - \mathbf{p}) - \hat{\mathbf{R}}^\top (\hat{\boldsymbol{\ell}} - \hat{\mathbf{p}}) \right) + \epsilon \quad (47e)$$

$$= \frac{\partial \mathbf{h}}{\partial {}^I \mathbf{p}_L} \hat{\mathbf{R}}^\top \left([\boldsymbol{\ell} - \mathbf{p}]_{\times} \tilde{\boldsymbol{\theta}} + \tilde{\boldsymbol{\ell}} - \tilde{\mathbf{p}} \right) + \epsilon \quad (47f)$$

$$\simeq \frac{\partial \mathbf{h}}{\partial {}^I \mathbf{p}_L} \hat{\mathbf{R}}^\top \left([\hat{\boldsymbol{\ell}} - \hat{\mathbf{p}}]_{\times} \tilde{\boldsymbol{\theta}} + \tilde{\boldsymbol{\ell}} - \tilde{\mathbf{p}} \right) + \epsilon \quad (47g)$$

$$= \mathbf{H} \tilde{\mathbf{x}} + \epsilon \quad (47h)$$

where

$$\mathbf{H} = \mathbf{\Pi} \mathbf{H}_e \quad (48)$$

$$\mathbf{\Pi} = \frac{\partial \mathbf{h}}{\partial {}^I \mathbf{p}_L} \mathbf{R}^\top \quad (49)$$

$$\mathbf{H}_e = \left[[\hat{\boldsymbol{\ell}} - \hat{\mathbf{p}}]_{\times} \quad -\mathbf{I}_3 \quad \mathbf{0} \quad \mathbf{0} \quad \mathbf{0} \quad \mathbf{I}_3 \right]. \quad (50)$$

We call \mathbf{H}_e the *essential measurement Jacobian*.

By combining (44) and (47), we obtain the linearized error-state system of VINS:

$$\begin{cases} \dot{\tilde{\mathbf{x}}} = \mathbf{F} \tilde{\mathbf{x}} + \mathbf{G} \mathbf{n} \\ \tilde{\mathbf{y}} = \mathbf{H} \tilde{\mathbf{x}} + \epsilon \end{cases} \quad (51)$$

5 Transformed Linearized Error-State System

5.1 Linear time-varying transformation on error-state

Denote the linear time-varying transformation by $\mathbf{T}(\tilde{\mathbf{x}})$, where $\mathbf{T}(\cdot)$ is a 18×18 nonsingular matrix function and remains to be chosen. The transformed error-state is obtained by multiplying the transformation with the original error-state:

$$\tilde{\mathbf{x}}^* = \mathbf{T}(\tilde{\mathbf{x}})\tilde{\mathbf{x}}. \quad (52)$$

For simplicity, the variable $\tilde{\mathbf{x}}$ of $\mathbf{T}(\tilde{\mathbf{x}})$ is omitted in the following if there is no ambiguity. Taking the derivative of both sides of (52) with respect to time, we have

$$\dot{\tilde{\mathbf{x}}}^* = \dot{\mathbf{T}}\tilde{\mathbf{x}} + \mathbf{T}\dot{\tilde{\mathbf{x}}}. \quad (53)$$

Substituting (52) and (53) into the linearized error-state system (51) yields the transformed linearized error-state system as follows

$$\begin{cases} \dot{\tilde{\mathbf{x}}}^* = \mathbf{F}^*\tilde{\mathbf{x}}^* + \mathbf{G}^*\mathbf{n} \\ \tilde{\mathbf{y}} = \mathbf{H}^*\tilde{\mathbf{x}}^* + \epsilon \end{cases} \quad (54)$$

where

$$\mathbf{F}^* = \dot{\mathbf{T}}\mathbf{T}^{-1} + \mathbf{T}\mathbf{F}\mathbf{T}^{-1} \quad (55)$$

$$\mathbf{G}^* = \mathbf{T}\mathbf{G} \quad (56)$$

$$\mathbf{H}^* = \mathbf{H}\mathbf{T}^{-1}. \quad (57)$$

According to (48) and (57), the essential measurement Jacobian \mathbf{H}_e is transformed into

$$\mathbf{H}_e^* = \mathbf{H}_e\mathbf{T}^{-1}. \quad (58)$$

The transformation is designed as follows:

$$\mathbf{T} = \begin{bmatrix} \mathbf{I}_3 & \mathbf{0} & \mathbf{0} & \mathbf{0} & \mathbf{0} & \mathbf{0} \\ [\hat{\mathbf{p}}]_x & \mathbf{I}_3 & \mathbf{0} & \mathbf{0} & \mathbf{0} & \mathbf{0} \\ [\hat{\mathbf{v}}]_x & \mathbf{0} & \mathbf{I}_3 & \mathbf{0} & \mathbf{0} & \mathbf{0} \\ \mathbf{0} & \mathbf{0} & \mathbf{0} & \mathbf{I}_3 & \mathbf{0} & \mathbf{0} \\ \mathbf{0} & \mathbf{0} & \mathbf{0} & \mathbf{0} & \mathbf{I}_3 & \mathbf{0} \\ [\hat{\boldsymbol{\epsilon}}]_x & \mathbf{0} & \mathbf{0} & \mathbf{0} & \mathbf{0} & \mathbf{I}_3 \end{bmatrix} \quad (59)$$

Correspondingly, its inverse and derivative are

$$\mathbf{T}^{-1} = \begin{bmatrix} \mathbf{I}_3 & \mathbf{0} & \mathbf{0} & \mathbf{0} & \mathbf{0} & \mathbf{0} \\ -[\hat{\mathbf{p}}]_{\times} & \mathbf{I}_3 & \mathbf{0} & \mathbf{0} & \mathbf{0} & \mathbf{0} \\ -[\hat{\mathbf{v}}]_{\times} & \mathbf{0} & \mathbf{I}_3 & \mathbf{0} & \mathbf{0} & \mathbf{0} \\ \mathbf{0} & \mathbf{0} & \mathbf{0} & \mathbf{I}_3 & \mathbf{0} & \mathbf{0} \\ \mathbf{0} & \mathbf{0} & \mathbf{0} & \mathbf{0} & \mathbf{I}_3 & \mathbf{0} \\ -[\hat{\boldsymbol{\theta}}]_{\times} & \mathbf{0} & \mathbf{0} & \mathbf{0} & \mathbf{0} & \mathbf{I}_3 \end{bmatrix} \quad (60)$$

$$\dot{\mathbf{T}} = \begin{bmatrix} \mathbf{0} & \mathbf{0} & \mathbf{0} & \mathbf{0} & \mathbf{0} & \mathbf{0} \\ [\hat{\mathbf{v}}]_{\times} & \mathbf{0} & \mathbf{0} & \mathbf{0} & \mathbf{0} & \mathbf{0} \\ [\hat{\mathbf{a}}]_{\times} & \mathbf{0} & \mathbf{0} & \mathbf{0} & \mathbf{0} & \mathbf{0} \\ \mathbf{0} & \mathbf{0} & \mathbf{0} & \mathbf{0} & \mathbf{0} & \mathbf{0} \\ \mathbf{0} & \mathbf{0} & \mathbf{0} & \mathbf{0} & \mathbf{0} & \mathbf{0} \\ \mathbf{0} & \mathbf{0} & \mathbf{0} & \mathbf{0} & \mathbf{0} & \mathbf{0} \end{bmatrix}. \quad (61)$$

The transformed Jacobians are

$$\mathbf{F}^* = \begin{bmatrix} \mathbf{0} & \mathbf{0} & \mathbf{0} & -\hat{\mathbf{R}} & \mathbf{0} & \mathbf{0} \\ \mathbf{0} & \mathbf{0} & \mathbf{I}_3 & -[\hat{\mathbf{p}}]_{\times} \hat{\mathbf{R}} & \mathbf{0} & \mathbf{0} \\ [\mathbf{g}]_{\times} & \mathbf{0} & \mathbf{0} & -[\hat{\mathbf{v}}]_{\times} \hat{\mathbf{R}} & -\hat{\mathbf{R}} & \mathbf{0} \\ \mathbf{0} & \mathbf{0} & \mathbf{0} & \mathbf{0} & \mathbf{0} & \mathbf{0} \\ \mathbf{0} & \mathbf{0} & \mathbf{0} & \mathbf{0} & \mathbf{0} & \mathbf{0} \\ \mathbf{0} & \mathbf{0} & \mathbf{0} & -[\hat{\boldsymbol{\theta}}]_{\times} \hat{\mathbf{R}} & \mathbf{0} & \mathbf{0} \end{bmatrix} \quad (62)$$

$$\mathbf{G}^* = \begin{bmatrix} -\hat{\mathbf{R}} & \mathbf{0} & \mathbf{0} & \mathbf{0} \\ -[\hat{\mathbf{p}}]_{\times} \hat{\mathbf{R}} & \mathbf{0} & \mathbf{0} & \mathbf{0} \\ -[\hat{\mathbf{v}}]_{\times} \hat{\mathbf{R}} & -\hat{\mathbf{R}} & \mathbf{0} & \mathbf{0} \\ \mathbf{0} & \mathbf{0} & \mathbf{I} & \mathbf{0} \\ \mathbf{0} & \mathbf{0} & \mathbf{0} & \mathbf{I} \\ -[\hat{\boldsymbol{\theta}}]_{\times} \hat{\mathbf{R}} & \mathbf{0} & \mathbf{0} & \mathbf{0} \end{bmatrix} \quad (63)$$

$$\mathbf{H}^* = \Pi \mathbf{H}_v^* \quad (64)$$

$$\mathbf{H}_e^* = \begin{bmatrix} \mathbf{0} & -\mathbf{I} & \mathbf{0} & \mathbf{0} & \mathbf{0} & \mathbf{I} \end{bmatrix} \quad (65)$$

5.2 Observability of the transformed system

Observability refers to the ability of a system to recover its initial states using all available measurements. The set of states that cannot be recovered from measurements constitutes the unobservable subspace of the system. For the system described in (54), we can utilize the local observability matrix [2, P. 180] to conduct

the observability analysis. Let \mathbf{M}^* denote the local observability matrix of system (51), then

$$\mathbf{M}^* = \begin{bmatrix} \mathbf{M}_0^* \\ \mathbf{M}_1^* \\ \vdots \\ \mathbf{M}_{n-1}^* \end{bmatrix} \quad (66)$$

where $\mathbf{M}_0 = \boldsymbol{\Pi} \mathbf{H}_e^*$ and

$$\mathbf{M}_{k+1}^* = \mathbf{M}_k^* \mathbf{F}^* + \dot{\mathbf{M}}_k^* \quad k = 0, 1, \dots, n-1. \quad (67)$$

According to (67), we can calculate

$$\mathbf{M}_1^* = \boldsymbol{\Pi} \mathbf{H}_e^* \mathbf{F}^* + \boldsymbol{\Pi}^{(1)} \mathbf{H}_e^* \quad (68)$$

$$\mathbf{M}_2^* = \boldsymbol{\Pi} \mathbf{H}_e^* \mathbf{F}^{*2} + \boldsymbol{\Pi}^{(1)} \mathbf{H}_e^* \mathbf{F}^* + \boldsymbol{\Pi}^{(1)} \mathbf{H}_e^* \mathbf{F}^* + \boldsymbol{\Pi} \mathbf{H}_e^* \mathbf{F}^{*(1)} + \boldsymbol{\Pi}^{(2)} \mathbf{H}_e^* \quad (69a)$$

$$= \boldsymbol{\Pi} (\mathbf{H}_e^* \mathbf{F}^{*2} + \boldsymbol{\Pi} \mathbf{H}_e^* \mathbf{F}^{*(1)}) + 2\boldsymbol{\Pi}^{(1)} \mathbf{H}_e^* \mathbf{F}^* + \boldsymbol{\Pi}^{(2)} \mathbf{H}_e^* \quad (69b)$$

The observability matrix is written as

$$\mathbf{M}^* = \begin{bmatrix} \boldsymbol{\Pi} & \mathbf{0} & \mathbf{0} \\ \boldsymbol{\Pi}^{(1)} & \boldsymbol{\Pi} & \mathbf{0} \\ \boldsymbol{\Pi}^{(2)} & 2\boldsymbol{\Pi}^{(1)} & \boldsymbol{\Pi} \end{bmatrix} \begin{bmatrix} \mathbf{H}_e^* \\ \mathbf{H}_e^* \mathbf{F}^* \\ \mathbf{H}_e^* \mathbf{F}^{*2} + \mathbf{H}_e^* \mathbf{F}^{*(1)} \end{bmatrix} \quad (70)$$

where

$$\begin{bmatrix} \mathbf{H}_e^* \\ \mathbf{H}_e^* \mathbf{F}^* \\ \mathbf{H}_e^* \mathbf{F}^{*2} + \mathbf{H}_e^* \mathbf{F}^{*(1)} \end{bmatrix} = \begin{bmatrix} \mathbf{0} & -\mathbf{I} & \mathbf{0} & \mathbf{0} & \mathbf{I} \\ \mathbf{0} & \mathbf{0} & -\mathbf{I} & \left[\hat{\mathbf{p}} - \hat{\boldsymbol{\ell}} \right] \times \hat{\mathbf{R}} & \mathbf{0} \\ -[\mathbf{g}]_\times & \mathbf{0} & \mathbf{0} & [\hat{\mathbf{v}}]_\times \hat{\mathbf{R}} + [\hat{\mathbf{v}}]_\times \hat{\mathbf{R}} + \left[\hat{\mathbf{p}} - \hat{\boldsymbol{\ell}} \right]_\times \hat{\mathbf{R}} [\hat{\omega}]_\times \hat{\mathbf{R}} & \mathbf{0} \end{bmatrix} \quad (71)$$

There exist four unobservable dimensions for the transformed linearized error-state system, s.t., $\mathbf{M}^* \mathbf{N}^* = \mathbf{0}$ with unobservable subspace

$$\mathbf{N}^* = \begin{bmatrix} \mathbf{0}_{3 \times 3} & \mathbf{g} \\ \mathbf{I}_3 & \mathbf{0}_{3 \times 1} \\ \mathbf{0}_{3 \times 3} & \mathbf{0}_{3 \times 1} \\ \mathbf{0}_{3 \times 3} & \mathbf{0}_{3 \times 1} \\ \mathbf{0}_{3 \times 3} & \mathbf{0}_{3 \times 1} \\ \mathbf{I}_3 & \mathbf{0}_{3 \times 1} \end{bmatrix}. \quad (72)$$

The unobservable subspace of the transformed system is independent of the state. When performing state estimation based on this transformed system, the erroneous reduction of unobservable dimensions is prevented, thus preserving consistency.

Remark 1. For $k > 2$, \mathbf{M}_k^* is complicated but does not affect our result about the observability. This is because only \mathbf{H}_e^* , $\mathbf{H}_e^* \mathbf{F}^*$, and $\mathbf{H}_e^* \mathbf{F}^{*2}$ contribute to observability analysis. If we continue to calculate \mathbf{M}_k^* when $k > 2$, the items such as $\mathbf{H}_e^* \mathbf{F}^{*m}$ and $\mathbf{H}_e^* \mathbf{F}^{*m} \mathbf{F}^{*(n)}$ will also be included in the left side of (71).

However, these terms only affect the blue-highlighted columns of (71). The nullspace blocks related to the blue-highlighted columns are always zeros, as shown in (72). Therefore, there is no need to calculate \mathbf{M}_k^* for $k > 2$.

6 Transformed Error-State Kalman Filter

In this section, we present the T-ESKF, a consistent VINS estimator based on the transformed linearized error-state system (54). The pipeline of T-ESKF is shown in Fig. 2.

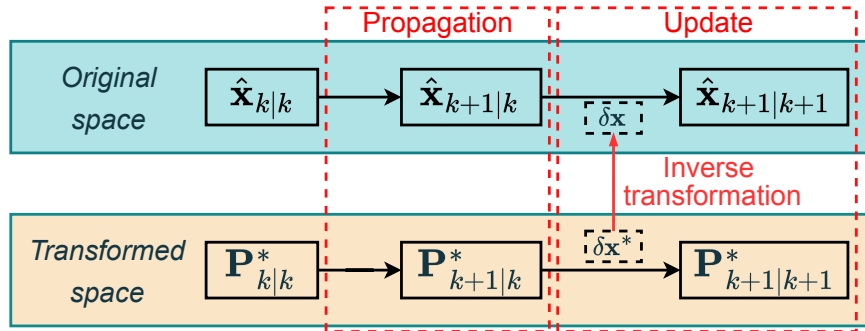


Figure 2: Pipeline of T-ESKF. It propagates and updates the covariance estimates in the transformed space. The state estimate is propagated by integrating (42) and updated using the state correction derived from the transformed system. The correction is obtained in the transformed space, and then transformed back to the original space.

6.1 Propagation

At each timestamp k , upon receiving a new IMU measurement, the state estimate at the previous time is propagated to the current time using either analytical integration [3] or the Runge-Kutta numerical integration of (42). Correspondingly, the transformed error-state covariance is propagated as follows:

$$\mathbf{P}_{k+1|k}^* = \Phi^*(t_{k+1}, t_k) \mathbf{P}_{k|k}^* \Phi^*(t_{k+1}, t_k)^\top + \mathbf{Q}_k^* \quad (73)$$

where the error-state transition matrix $\Phi^*(t_{k+1}, t_k)$ is computed by integrating the differential equation

$$\dot{\Phi}^*(\tau, t_k) = \mathbf{F}^* \Phi^*(\tau, t_k) \quad (74)$$

with the initial condition $\Phi^*(t_k, t_k) = \mathbf{I}_{18}$. The noise propagation matrix is computed by

$$\mathbf{Q}_k^* = \int_{t_k}^{t_{k+1}} \Phi^*(t_{k+1}, \tau) \mathbf{G}_\tau^* \mathbf{Q} \mathbf{G}_\tau^{*\top} \Phi^*(t_{k+1}, \tau)^\top d\tau. \quad (75)$$

Since T-ESKF share the same linearized error-state system with RI-EKF, we can analytical integrate

$\Phi^*(t_{k+1}, t_k)$ and \mathbf{Q}_k^* as [4]:

$$\Phi^*(t_{k+1}, t_k) = \begin{bmatrix} \mathbf{I}_3 & \mathbf{0} & \mathbf{0} & -\hat{\mathbf{R}}_{k|k}\mathbf{J}_l(\hat{\omega}_k\Delta t)\Delta t & \mathbf{0} & \mathbf{0} \\ \left[\frac{1}{2}\mathbf{g}\Delta t^2\right]_{\times} & \mathbf{I}_3 & \mathbf{I}_3\Delta t & -\left[\hat{\mathbf{p}}_{k+1|k}\right]_{\times}\hat{\mathbf{R}}_{k|k}\mathbf{J}_l(\hat{\omega}_k\Delta t)\Delta t + \hat{\mathbf{R}}_{k|k}\Xi_4 & -\hat{\mathbf{R}}_{k|k}\Xi_2 & \mathbf{0} \\ [\mathbf{g}\Delta t]_{\times} & \mathbf{0} & \mathbf{I}_3 & -\left[\hat{\mathbf{v}}_{k+1|k}\right]_{\times}\hat{\mathbf{R}}_{k|k}\mathbf{J}_l(\hat{\omega}_k\Delta t)\Delta t + \hat{\mathbf{R}}_{k|k}\Xi_3 & -\hat{\mathbf{R}}_{k|k}\Xi_1 & \mathbf{0} \\ \mathbf{0} & \mathbf{0} & \mathbf{0} & & \mathbf{0} & \mathbf{0} \\ \mathbf{0} & \mathbf{0} & \mathbf{0} & & & \mathbf{I}_3 \\ \mathbf{0} & \mathbf{0} & \mathbf{0} & -\left[\hat{\boldsymbol{\theta}}_{k+1|k}\right]_{\times}\hat{\mathbf{R}}_{k|k}\mathbf{J}_l(\hat{\omega}_k\Delta t)\Delta t & \mathbf{0} & \mathbf{I}_3 \end{bmatrix} \quad (76)$$

$$\mathbf{Q}_k^* = \mathbf{G}_k^*\mathbf{Q}\mathbf{G}_k^{*\top} \quad (77)$$

$$\mathbf{G}_k^* = \begin{bmatrix} -\hat{\mathbf{R}}_{k|k}\mathbf{J}_l(\hat{\omega}_k\Delta t)\Delta t & \mathbf{0} & \mathbf{0} & \mathbf{0} \\ -\left[\hat{\mathbf{P}}_{k+1|k}\right]_{\times}\hat{\mathbf{R}}_{k|k}\mathbf{J}_l(\hat{\omega}_k\Delta t)\Delta t + \hat{\mathbf{R}}_{k|k}\Xi_4 & -\hat{\mathbf{R}}_{k|k}\Xi_2 & \mathbf{0} & \mathbf{0} \\ -\left[\hat{\mathbf{v}}_{k+1|k}\right]_{\times}\hat{\mathbf{R}}_{k|k}\mathbf{J}_l(\hat{\omega}_k\Delta t)\Delta t + \hat{\mathbf{R}}_{k|k}\Xi_3 & -\hat{\mathbf{R}}_{k|k}\Xi_1 & \mathbf{0} & \mathbf{0} \\ \mathbf{0} & \mathbf{0} & \mathbf{I}_3\Delta t & \mathbf{0} \\ \mathbf{0} & & \mathbf{0} & \mathbf{I}_3\Delta t \\ -\left[\hat{\boldsymbol{\theta}}_{k+1|k}\right]_{\times}\hat{\mathbf{R}}_{k|k}\mathbf{J}_l(\hat{\omega}_k\Delta t)\Delta t & \mathbf{0} & \mathbf{0} & \mathbf{0} \end{bmatrix} \quad (78)$$

where $\Delta t = t_{k+1} - t_k$,

$$\Xi_1 \triangleq \int_{t_k}^{t_{k+1}} \text{Exp}(\hat{\boldsymbol{\omega}}(\tau - t_k)) d\tau \quad (79a)$$

$$\Xi_2 \triangleq \int_{t_k}^{t_{k+1}} \int_{t_k}^s \text{Exp}(\hat{\boldsymbol{\omega}}(\tau - t_k)) d\tau ds \quad (79b)$$

$$\Xi_3 \triangleq \int_{t_k}^{t_{k+1}} \text{Exp}(\hat{\boldsymbol{\omega}}(\tau - t_k)) [\hat{\mathbf{a}}_k]_{\times} \mathbf{J}_r(\hat{\boldsymbol{\omega}}(\tau - t_k))(\tau - t_k) d\tau \quad (79c)$$

$$\Xi_4 \triangleq \int_{t_k}^{t_{k+1}} \int_{t_k}^s \text{Exp}(\hat{\boldsymbol{\omega}}_k(\tau - t_k)) [\hat{\mathbf{a}}_k]_{\times} \mathbf{J}_r(\hat{\boldsymbol{\omega}}_k(\tau - t_k))(\tau - t_k) d\tau ds \quad (79d)$$

The computations of Ξ_1 , Ξ_2 , Ξ_3 , and Ξ_4 are detailed in [Openvins: Analytical Integration Components](#).

6.2 Update

In T-ESKF, the transformed measurement Jacobian is evaluated at the current best state estimate $\hat{\mathbf{x}}_{k+1|k}$:

$$\mathbf{H}_{k+1}^* = \Pi|_{\mathbf{x}=\hat{\mathbf{x}}_{k+1|k}} \mathbf{H}_e^*. \quad (80)$$

The Kalman gain can be then computed following the classical EKF:

$$\mathbf{K}^* = \mathbf{P}_{k+1|k}^* \mathbf{H}_{k+1}^{*\top} (\mathbf{H}_{k+1}^* \mathbf{P}_{k+1|k}^* \mathbf{H}_{k+1}^{*\top} + \mathbf{V})^{-1}. \quad (81)$$

By using the Kalman gain, the state correction in the transformed space can be obtained as follows:

$$\delta \mathbf{x}^* = \mathbf{K}^* \tilde{\mathbf{y}}_{k+1}. \quad (82)$$

Correspondingly, the covariance is updated by

$$\mathbf{P}_{k+1|k+1}^* = \mathbf{P}_{k+1|k}^* - \mathbf{K}^* \mathbf{H}_{k+1}^* \mathbf{P}_{k+1|k}^*. \quad (83)$$

6.3 Inverse transformation

Note that $\delta\mathbf{x}^*$ is the state correction expressed in the transformed space. To update the state estimate, we need to inversely transform the state correction from the transformed space to the original space:

$$\delta\mathbf{x} = \mathbf{T}(\hat{\mathbf{x}}_{k+1|k})^{-1} \delta\mathbf{x}^*. \quad (84)$$

Then the state estimate can be updated as follows:

$$\hat{\mathbf{x}}_{k+1|k+1} = \hat{\mathbf{x}}_{k+1|k} \oplus \delta\mathbf{x} = \begin{pmatrix} \text{Exp}(\delta\boldsymbol{\theta}) \hat{\mathbf{R}}_{k+1|k} \\ \hat{\mathbf{p}}_{k+1|k} + \delta\mathbf{p} \\ \hat{\mathbf{v}}_{k+1|k} + \delta\mathbf{v} \\ \hat{\mathbf{b}}_{g,k+1|k} + \delta\mathbf{b}_g \\ \hat{\mathbf{a}}_{g,k+1|k} + \delta\mathbf{b}_a \\ \hat{\boldsymbol{\ell}}_{k+1|k} + \delta\boldsymbol{\ell} \end{pmatrix}. \quad (85)$$

6.4 Initialization

Before T-ESKF operates, the initial state estimate $\hat{\mathbf{x}}_{0|0}$ and the covariance $\mathbf{P}_{0|0}$ can be acquired based on prior information. The covariance associated with the transformed error-state is obtained through the transformation of the initial covariance:

$$\mathbf{P}_{0|0}^* = \mathbf{T}(\hat{\mathbf{x}}_{0|0}) \mathbf{P}_{0|0} \mathbf{T}(\hat{\mathbf{x}}_{0|0})^\top. \quad (86)$$

7 Real-World Experiments

In addition to the dataset experiments, we further compare T-ESKF with T-ESKF with ESKF [1], FEJ-ESKF [5], and RI-EKF [6] using our custom sensor platform mounted on an aerial robot, as depicted in Figure 3. This platform provides stereo images at 30Hz with a resolution of 848×480 and IMU data at 200Hz, with the main parameters outlined in Table 1. The camera intrinsics and extrinsics parameters are calibrated using the offline calibration toolbox Kalibr. For robust performance, camera intrinsics and time offset calibrations are enabled.

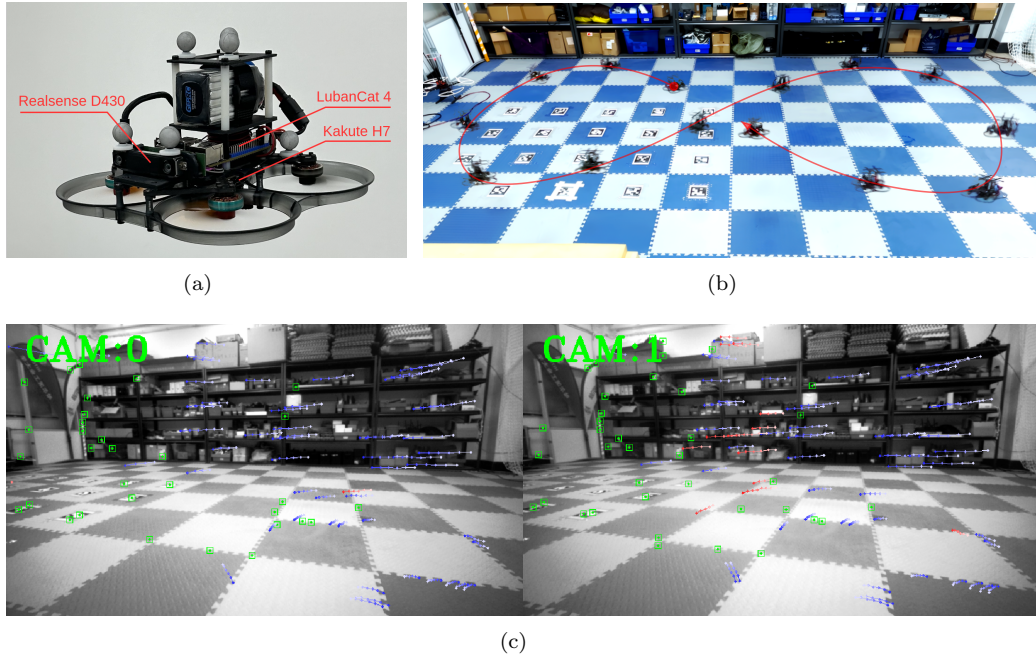


Figure 3: (a) Aerial robot with a Realsense D430 stereo camera, a Kakute H7 flight controller (MPU6000), and an onboard computer, LubanCat 4. (b) Figure-eight flight trajectory with unfixed yaw. (c) A sample frame with tracked features in the experiment.

Table 1: Real-world experiment configuration

Parameter	Value	Parameter	Value
Accel. White Noise	6.33e-03	Gyro White Noise	8.71e-04
Accel. Random Walk	2.87e-03	Gyro Random Walk	3.34e-05
Pixel Noise	1	IMU Freq.	200
Max Cam Pts/Frame	200	Cam Freq.	30
Max Feats/Frame	60	Cam Number	Stereo
Max Clone Size	11	Feat. Rep.	Global XYZ

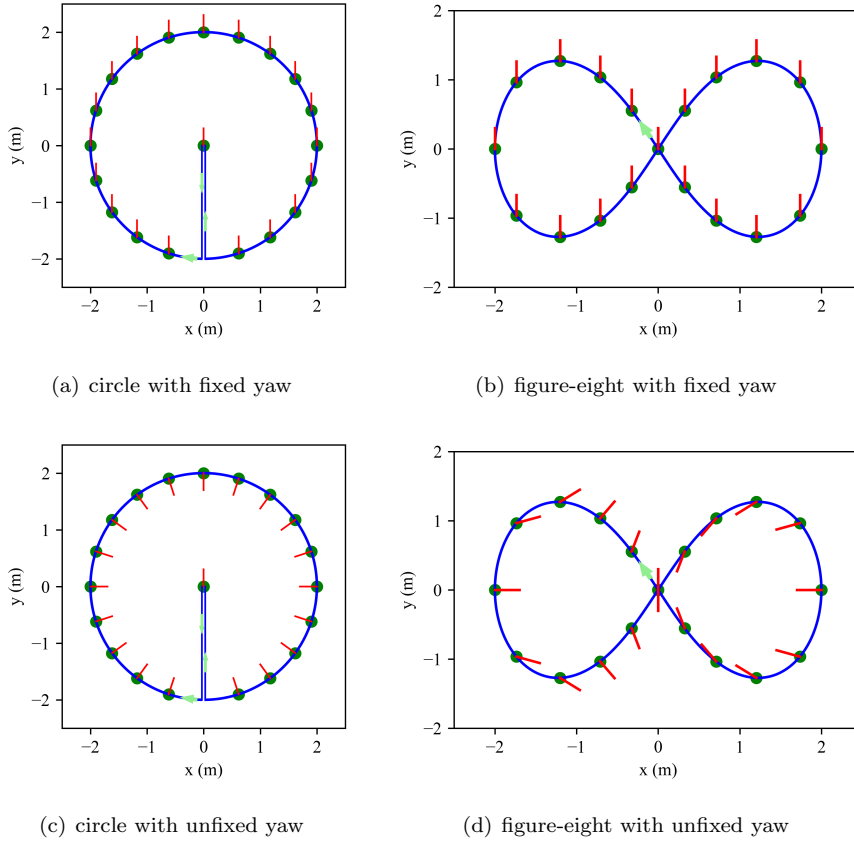


Figure 4: Designed trajectories in real-world experiments. The circle or the figure-eight pattern is repeated 6 times in each trajectory. The red lines represent the orientation of the aerial robot. The lightgreen arrows indicate the direction of the trajectories.

The aerial robot is commanded to follow either a circular or a figure-eight trajectory with fixed or unfixed yaw, as illustrated in Figure 4. The time taken to track a circle is 6.28 seconds, and for a figure-eight, it is 10.47 seconds. Each trajectory includes six repetitions of the circular or figure-eight patterns. Three datasets are gathered for each scenario, consisting of IMU and stereo camera measurements, in addition to groundtruth acquired from the motion capture system.

To evaluate the estimated results, we align the estimated trajectories and the ground truth based on the initial frame, as depicted in Figure 5. The RMSE of these estimators is detailed in Table 2. As seen, the performance of these estimators is close when the yaw is fixed. Nonetheless, T-ESKF surpasses ESKF, particularly in orientation estimation. In the case of unfixed yaw, T-ESKF exhibits superior performance compared to ESKF and FEJ-ESKF.

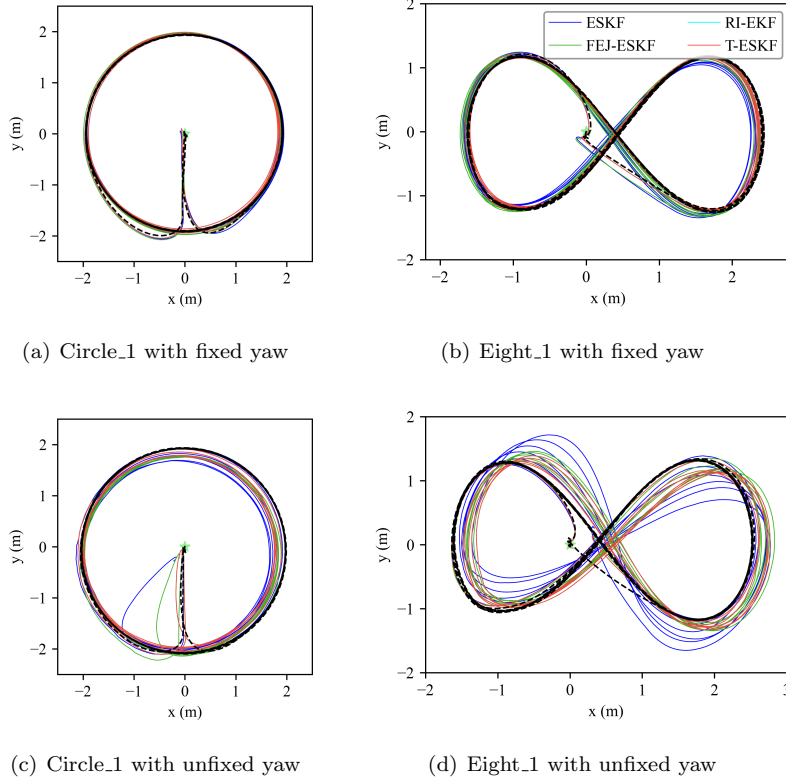


Figure 5: Estimated trajectories on the first dataset in each case. The black dashed line is the groundtruth trajectory with a green star marking the starting point. The estimated trajectories are aligned to the groundtruth trajectory (black dashed line) using the beginning frame.

Table 2: Average orientation (deg) and position (meter) NEES of 100 Monte-Carlo simulation runs under various measurement noise levels

	Set	ESKF	FEJ-ESKF	RI-EKF	T-ESKF
Fixed yaw	Circle_1	1.432 / 0.066	1.261 / 0.054	1.270 / 0.061	1.270 / 0.061
	Circle_2	1.236 / 0.057	1.492 / 0.059	1.114 / 0.047	1.113 / 0.047
	Circle_3	5.309 / 0.165	1.469 / 0.076	1.216 / 0.068	1.198 / 0.075
	Eight_1	2.333 / 0.114	1.017 / 0.085	0.878 / 0.058	0.878 / 0.058
	Eight_2	3.882 / 0.142	1.884 / 0.133	1.539 / 0.135	1.434 / 0.126
	Eight_3	2.885 / 0.105	1.373 / 0.100	1.148 / 0.096	0.940 / 0.103
	Average	2.846 / 0.108	1.416 / 0.084	1.194 / 0.078	1.139 / 0.078
Unfixed yaw	Circle_1	26.617 / 0.665	11.655 / 0.402	2.734 / 0.128	2.747 / 0.128
	Circle_2	25.674 / 0.727	2.334 / 0.104	2.180 / 0.137	2.180 / 0.137
	Circle_3	25.023 / 0.689	2.056 / 0.134	2.633 / 0.124	1.555 / 0.125
	Eight_1	12.833 / 0.366	4.712 / 0.245	3.702 / 0.216	3.716 / 0.216
	Eight_2	12.447 / 0.397	6.360 / 0.349	6.456 / 0.277	6.138 / 0.273
	Eight_3	15.979 / 0.440	6.534 / 0.355	6.440 / 0.368	6.438 / 0.368
	average	19.762 / 0.547	5.609 / 0.265	4.024 / 0.208	3.796 / 0.208

A Derivation of $\mathbf{C}_2 = [\mathbf{g}]_\times$

To make the derivation easy to read, we recall some equations first:

$$\mathbf{C}_1 = \dot{\mathbf{T}}_{\mathbf{p}} - \mathbf{T}_{\mathbf{v}} \quad (87)$$

$$\mathbf{C}_2 = \dot{\mathbf{T}}_{\mathbf{v}} - [\hat{\mathbf{R}}\mathbf{a}_m]_\times \quad (88)$$

$$\mathbf{C}_3 = \dot{\mathbf{T}}_{\boldsymbol{\epsilon}} \quad (89)$$

$$\mathbf{C}_4 = [\hat{\boldsymbol{\epsilon}} - \hat{\mathbf{p}}]_\times + \mathbf{T}_{\mathbf{p}} - \mathbf{T}_{\boldsymbol{\epsilon}} \quad (90)$$

Note that $(\mathbf{C}_1, \mathbf{C}_2, \mathbf{C}_3, \mathbf{C}_4)$ are constant matrices. Taking the derivative of (87) and (89) and the second order derivative of (90), we have

$$\mathbf{0} = \ddot{\mathbf{T}}_{\mathbf{p}} - \dot{\mathbf{T}}_{\mathbf{v}} \quad (91)$$

$$\mathbf{0} = \ddot{\mathbf{T}}_{\boldsymbol{\epsilon}} \quad (92)$$

$$\mathbf{0} = -[\hat{\mathbf{a}}]_\times + \ddot{\mathbf{T}}_{\mathbf{p}} - \ddot{\mathbf{T}}_{\boldsymbol{\epsilon}} \quad (93)$$

By combining these equations with (88)+(91)-(92)-(93), we get \mathbf{C}_2 :

$$\mathbf{C}_2 = [\hat{\mathbf{a}} - \hat{\mathbf{R}}\mathbf{a}_m]_\times = [\mathbf{g}]_\times. \quad (94)$$

References

- [1] J. Sola, “Quaternion kinematics for the error-state kalman filter,” *arXiv preprint arXiv:1711.02508*, 2017.
- [2] C.-T. Chen, *Linear System Theory and Design*. The Oxford Series in Electrical and Computer Engineering, New York Oxford: Oxford University Press, 3. ed., 3. print ed., 1999.
- [3] Y. Yang, B. P. Wisely Babu, C. Chen, G. Huang, and L. Ren, “Analytic combined imu integration (aci2) for visual inertial navigation,” in *2020 IEEE International Conference on Robotics and Automation (ICRA)*, pp. 4680–4686, 2020.
- [4] Y. Yang, C. Chen, W. Lee, and G. Huang, “Decoupled Right Invariant Error States for Consistent Visual-Inertial Navigation,” *IEEE Robotics and Automation Letters*, vol. 7, pp. 1627–1634, Apr. 2022.
- [5] G. P. Huang, A. I. Mourikis, and S. I. Roumeliotis, “Analysis and improvement of the consistency of extended Kalman filter based SLAM,” in *2008 IEEE International Conference on Robotics and Automation*, pp. 473–479, May 2008.
- [6] T. Zhang, K. Wu, J. Song, S. Huang, and G. Dissanayake, “Convergence and consistency analysis for a 3-D Invariant-EKF SLAM,” *IEEE Robotics and Automation Letters*, vol. 2, pp. 733–740, Apr. 2017.